Ref. Ares(2020)7633550 - 15/12/2020

H2020

D4.6 2D SPECTROMETER AND IMAGING OPTICS

FLAIR - FLying ultrA-broadband single-shot InfraRed Sensor
GA732968

Deliverable Information	
Deliverable Number: D4.6	**Work Package: WP4**
Date of Issue: 21/11/2020	
Document Reference: 732968-FLAIR-D4.6 2D spectrometer and imaging optics	
Version Number: 1.0	
Nature of Deliverable: Demonstrator	**Dissemination Level of Deliverable:** PU
Author(s): Sanghoon CHIN, Laurent BALET	
Keywords: 2D, spectrometer, VIPA, grating	

Abstract:
This document constitutes the technical report for FLAIR demonstrator deliverable D4.6 and reports on the design and performance of 3 different types of spectrometers that have been developed with the goal of UAV integration during this project at CSEM.

Document History

Date	Version	Remarks
10/03/2020	0.1	Skeleton
11/03/2020	0.2	First draft document
22/11/2020	0.2	Document ready for review by the coordinator
02/12/2020	1.0	Final version for uploading on the EU server

Document Authors

Entity	Contributors
CSEM SA	Sanghoon CHIN Fabian LÜTOLF Julien GOUMAN Laurent BALET

Disclosure Statement: The information contained in this document is the property of FLAIR Consortium and it shall not be reproduced, disclosed, modified or communicated to any third parties without the prior written consent of the abovementioned entities.

Executive Summary

This document reports on Task 4.6 of the FLAIR project, concerned with the design of breadboard-based 2D spectrometer and imaging optics that could be integrated in a UAV or other flying platforms. Using the broadband supercontinuum light source from NKT Photonics with a maximum intensity at 3.25 µm and the infrared 2D matrix detector from NIT, 3 different types of spectrometers have been developed. This unscheduled number of developed systems has been necessary to finally reach the performances satisfying the requirements of the FLAIR sensor system.

Table of Contents

List of Tables

List of Figures

List of Acronyms

Acronym	Meaning
FLAIR	FLying ultrA-broadband single-shot InfraRed Sensor
IR	Infrared
NUC	Non-Uniformity Correction
MIR	mid-infrared
MPC	multipass cell
ppm	Particle per million
OAP	Off-axis parabolic mirror
SC	Supercontinuum
SNR	Signal-to-noise ratio
VIPA	Virtual Imaged Phased Array

Table 1: List of acronyms.

1 Introduction

FLAIR is an air quality sensing system for sensitive and selective detection of molecular fingerprints in the mid-infrared atmospheric window. Figure 1 depicts the entire FLAIR system, at which the position and role of 2D spectrometer and imaging optics are briefly illustrated.

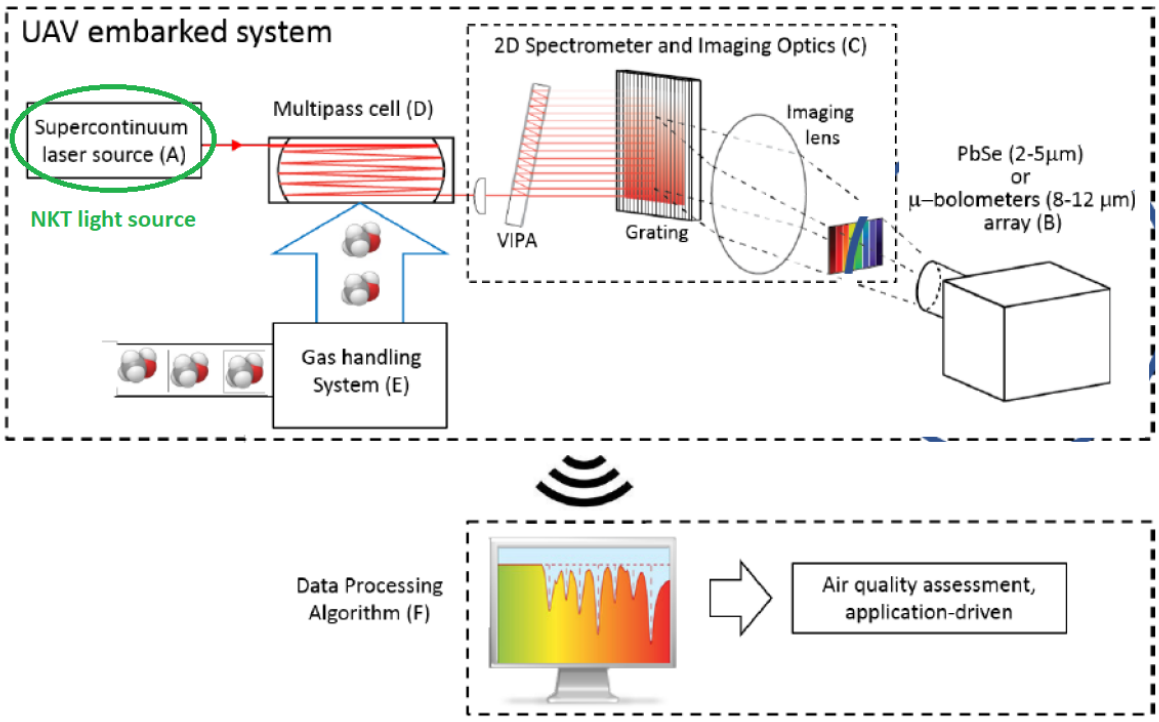

Figure 1: Block diagram showing the position of NKT's light source in the FLAIR system.

The initial design of 2D spectrometer relied on the combination of two dispersion elements: a VIPA (Virtual Imaged Phase Array) and a diffraction grating. This configuration is a compact and efficient geometrical method to spectrally disperse a broadband light source into 2 orthogonal directions, hence, resulting in a 2-dimensional dispersion spectrum on a matrix detector. It is often found in astronomy in conjunction with highly sensitive cooled detectors. However, it turned out that the limit of detection down to the ppm level could not be reached with this system. The cause is an insufficient signal to noise ratio, which can be attributed to a conjunction of three parameters: 1) the total optical loss through such a spectrometer are practically too large, 2) the relative intensity noise of the light source is high, 3) The fixed-pattern noise of the camera is very high, limiting the detection sensitivity of the sensor. Following a decision of the consortium, it has been decided to keep the light source, which is the state of the art in this wavelength region. It has also decided to continue working with the uncooled 2D vapor phase deposited PbSe on Si-CMAOS substrate developed by NIT specially for this project. For this reason, the VIPA approach had to be put aside.
The 3 different types of spectrometers (including the initial design) that have been developed are presented in the following section, and their performance such as sensitivity and spectral resolution will be reported.

1.1 Requirements

The main requirements for the spectrometer developed within this project where

1. Robustness, compactness, low weight and low power consumption of the system to be compatible with UAV or other airborne operation
2. Detection limit down to the ppm level for species of interest, like *e.g.* methane

3. Single shot spectral window larger than 30 cm^{-1} with a spectral resolution better than 1 cm^{-1} near the Q-branch absorption region of methane to ensure a good discrimination between multiple species by the analysis algorithm.

2 2D spectrometer and imaging optics

The different types of spectrometer have been modelled in Zemax, whenever needed, and then assembled on our optical tables for testing their real performances.

2.1 VIPA-based spectrometer

2.1.1 Principle and Setup

The baseline of the project was to use a cross-dispersed spectrometer to produce 2D absorption spectra on the 128 x 128 pixel NIT camera.

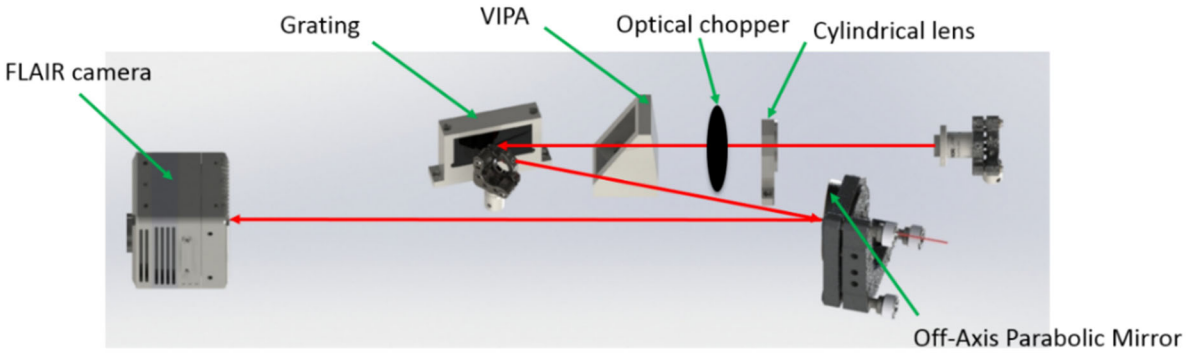

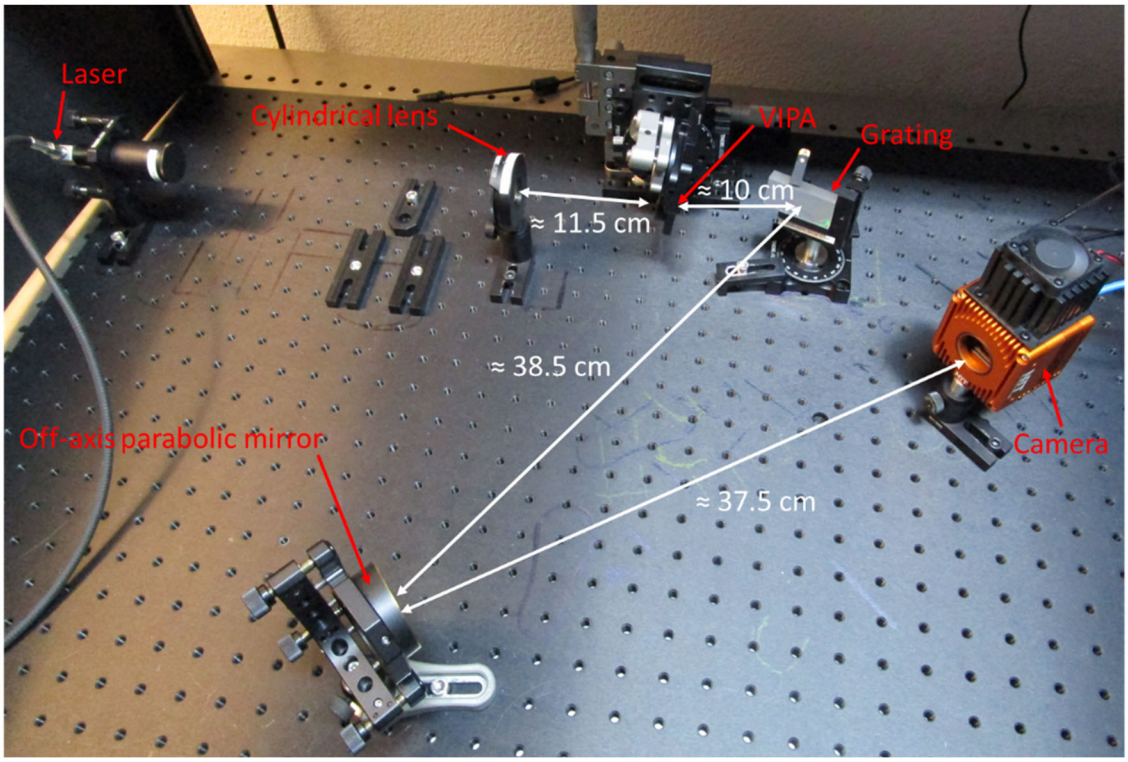

Figure 2: VIPA based 2D spectrometer setup. (top) sketch (bottom) laboratory realization.

The laboratory version of the VIPA based 2-dimensional spectrometer, as pictured in Figure 2, is composed of the SC source (NKT, first delivered MIR system) connected to a reflective collimator (Thorlabs RC04APC-P01), followed by an optical bandpass filter (e.g IWBP3700-

4500). The purpose of the filter is to narrow the optical spectrum to avoid the overlapping of higher order modes dispersed by the VIPA on the detector, and to absorb the remaining seed laser at 1.6 µm. The gas cells can then be placed on the collimated portion of the beam. Alternatively, a flip mirror can be actioned to direct the light towards the MPC, once it will be delivered (Figure 3).

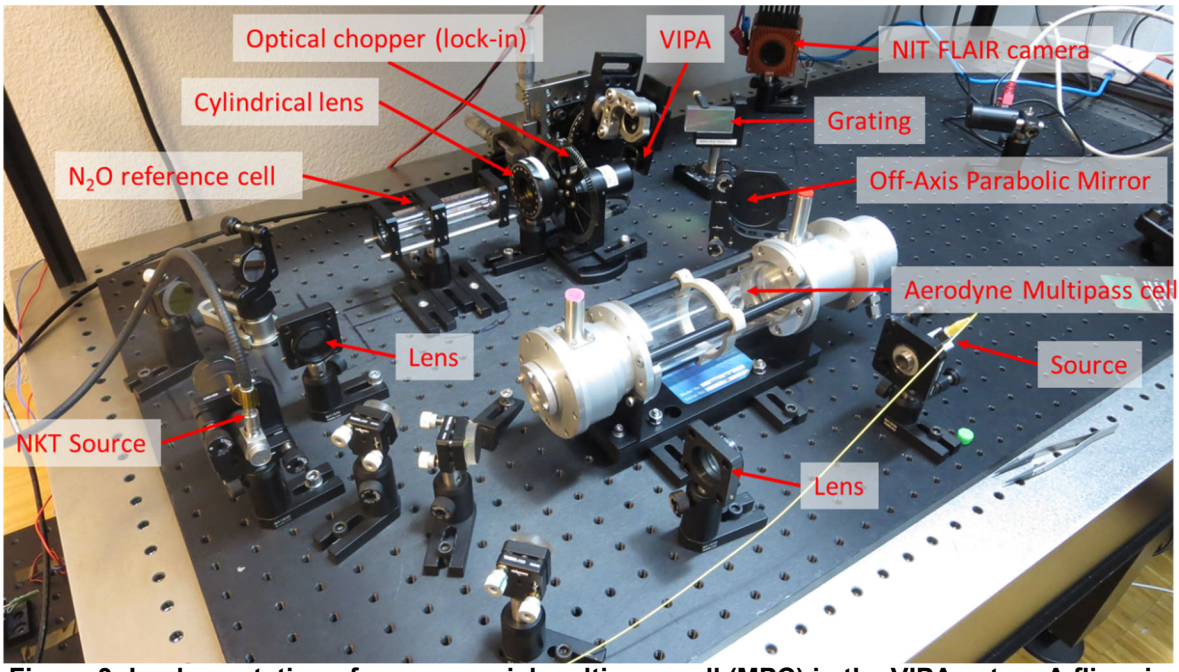

Figure 3: Implementation of a commercial multipass cell (MPC) in the VIPA setup. A flip mirror can select between the calibrated gas cells or the MPC.

A cylindrical lens (Thorlabs LJ5027RM-E) focusses the beam on the VIPA (Lightmachinery, Inc. OP-7553-3000-1 Rev A). A portion of the vertically dispersed light is then dispersed horizontally by a ruled reflective diffraction grating (Thorlbas GR2550-30035). A metallic off-axis parabolic mirror (Thorlbas MPD2151-M01) images the 2D dispersed spectrum on the NIT PbSe Camera developed within the frame of the project.

2.1.2 Experimental results

Absorption measurement performed on 10 cm long N_2O and CH_4 reference cells with various pressures, and extrapolated to a lossless, 10 m long path length, indicate a detection limit between 100 and 250 ppm for N_2O, and above 5000 ppm for CH_4. The detection limit for methane has been estimated in a spectral region where methane and nitrous oxide have overlapping absorption spectra, but away from the Q-branch. The detection limit might be slightly improved (up to a factor 10) when targeting the 3.3 µm region but remains some orders of magnitude too high for testing the prototype in outside environmental conditions.
The spectral coverage (35.1cm^{-1}) and resolution (0.1cm^{-1}) have been estimated based on HITRAN simulations (see Figure 4) and are within specifications.

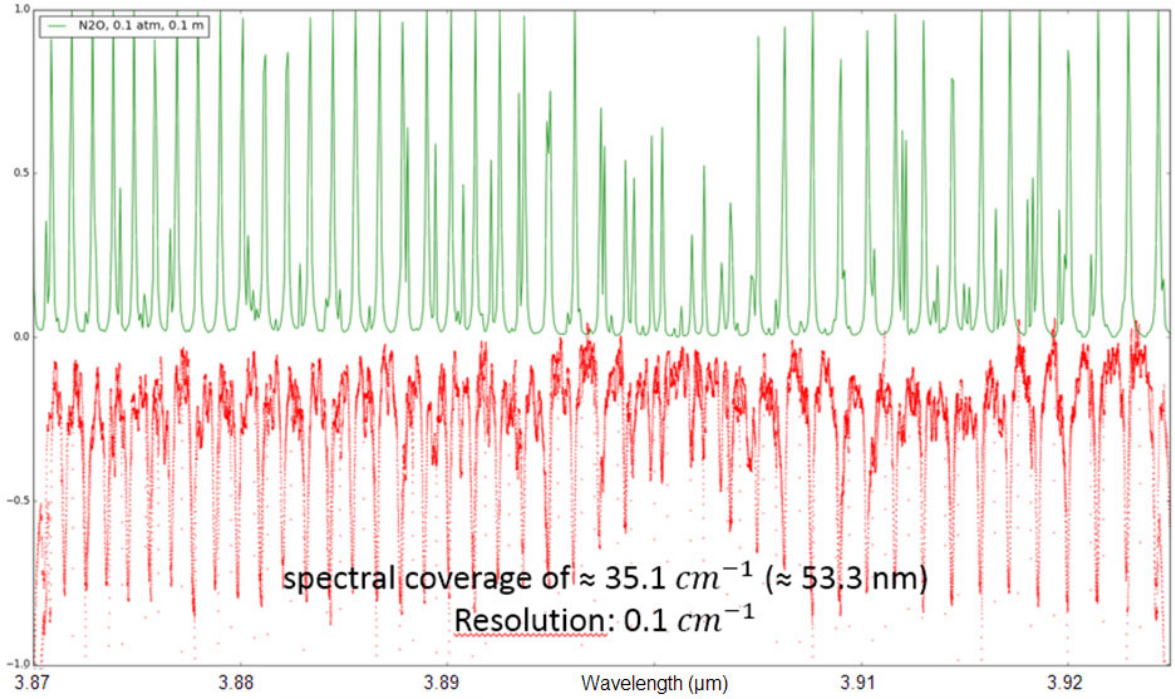

Figure 4: Comparison between HITRAN simulated absorption spectrum (top, green) and actual measurement on N2O reference cell (bottom, red) indicate a spectral coverage of 35.1 cm^{-1} and an excellent spectral resolution of 0.1 cm^{-1}.

Such absorption spectra are extracted from the 2D dispersion pattern as recorded by the NIT camera (See Figure 5(left)), where each diagonal line visible on the figure corresponds to a portion of the spectrum. Figure 5(right) illustrates how the final linear spectrum is obtained by concatenating several of those lines. The different colors help understand the process as each corresponds to a diagonal line from the left picture. The 2D spectrum optimally fills the 2D detector array, with some redundancy, and no unused pixels. A slight overlap between the lines is visible, indicating that no portion of the spectrum is lost. With a better choice of imaging optics (not off-the-shelf) the spectral window could be slightly expanded.

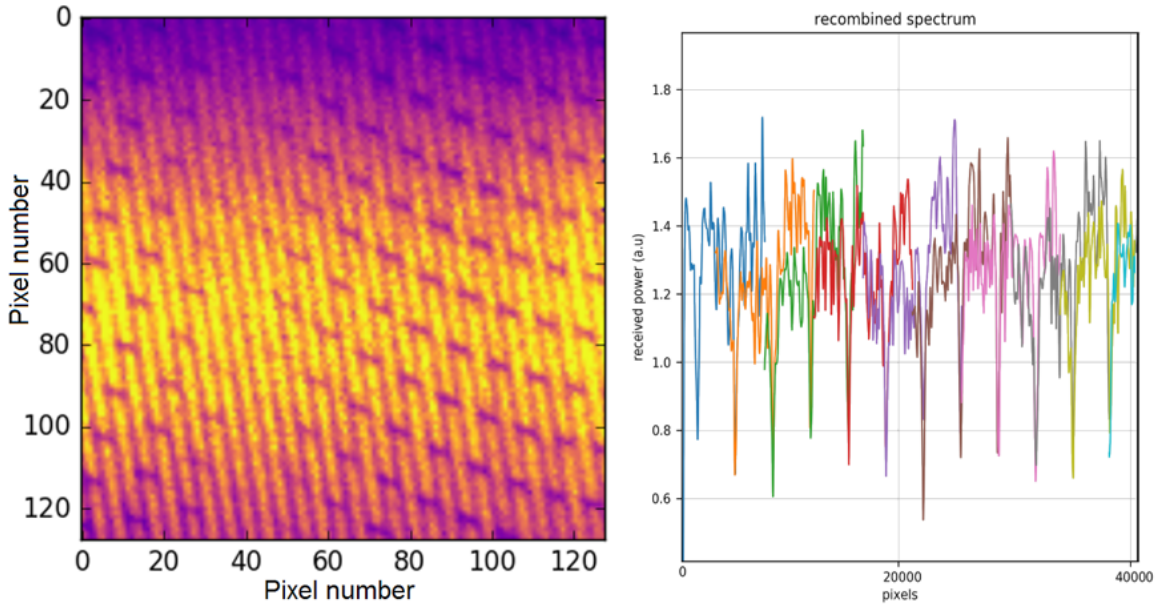

Figure 5: (left) example 2D absorption spectrum of N_2O recorded on the NIT camera, and (left) linearization of the 2D spectrum line by line, with each line shown in different color for clarity.

Despite its excellent resolution and sufficient spectral coverage, the VIPA based setup did not complied with the required detection limit.
On the mechanical aspect, the VIPA as a large mass compared to other optics and could be more sensitive to acceleration and vibration. The alignment is quite sensitive, as the light source must be focussed tightly to a line matching closely the entrance window of the VIPA. We also had an incident where the optical surface delaminated from the substrate for an unknown cause, probably related to humidity.
All those reasons lead us to explore alternative designs.

2.2 Echelle grating-based spectrometer

2.2.1 Principle and Setup

Due to the limited sensitivity of VIPA-based spectroscopy, CSEM decided to construct another 2D spectrometer inspired by R.A.Probst *et al.* in Appl. Phys. B, 123:76 (2017). It makes use of the combination of one echelle grating and one normal grating, as shown in **Figure 6** (schematic diagram) and

Figure 8 (experimental setup). The principle of this echelle grating-based spectroscopy is very similar to the VIPA-based one. An advantage of echelle grating over the VIPA, in addition to the ease of alignment, is the smaller optical power loss; hence leading to a better signal-to-noise ratio, but it is at the cost of slightly larger spectral resolution.

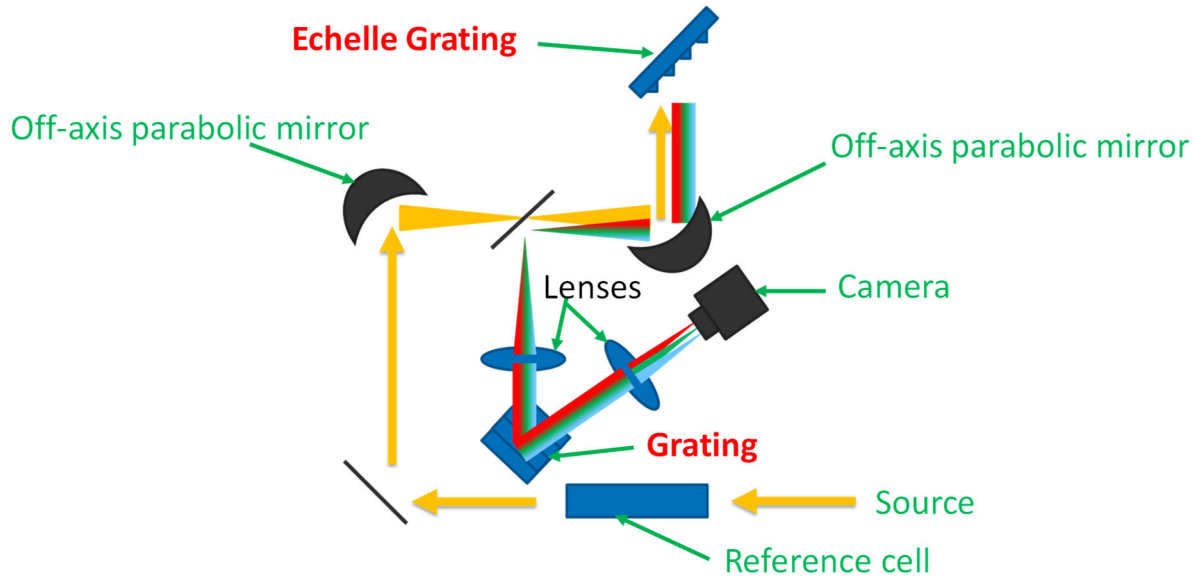

Figure 6: Sketch illustrating the working principle of the crossed-grating 2D spectrometer.

Figure 7 shows a sketch and the Zemax model of the version implemented at CSEM: The beam coming from the multi-pass cell is collimated, before being focused by a 90° off-axis parabolic mirror, re-collimated by a second 90° off-axis parabolic mirror and finally directed to the Echelle grating. The grating is illuminated in Littrow configuration to minimize losses, meaning that the diffracted light travels exactly in the opposite direction of the incoming light. The specific mirror configuration has the advantage that the diffracted light can easily be extracted close to the focus point of the off-axis mirrors by placing a flat 45° mirror right next to the focus while slightly rotating the grating around its surface normal. Mirrors and grating have been chosen such that at least 2 orders of the central wavelength are extracted (see zoom on the Zemax model).

The extracted light is then collimated by a lens before being cross-dispersed by the second grating, and then focussed on the camera with the Fourier lens. The setup was assembled and aligned with a visible laser and subsequently tested with a supercontinuum from NKT.

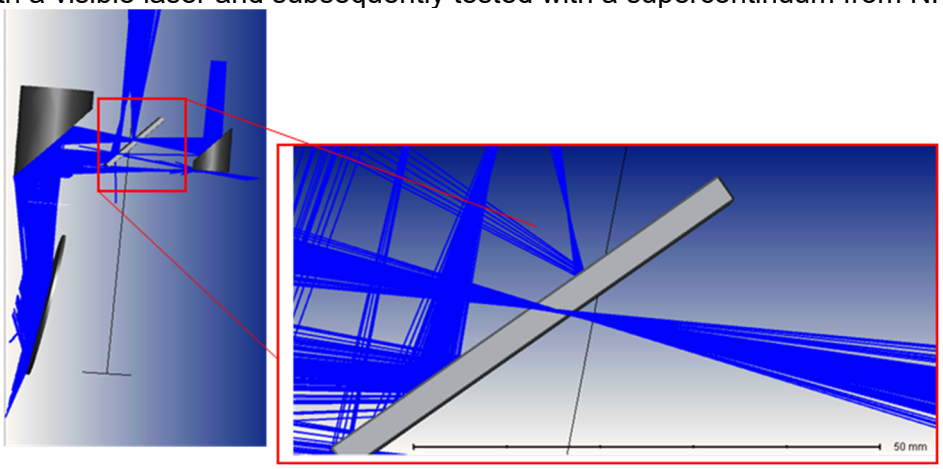

Figure 7: Zemax model used to validate the sketched concept.

2.2.2 Experimental results

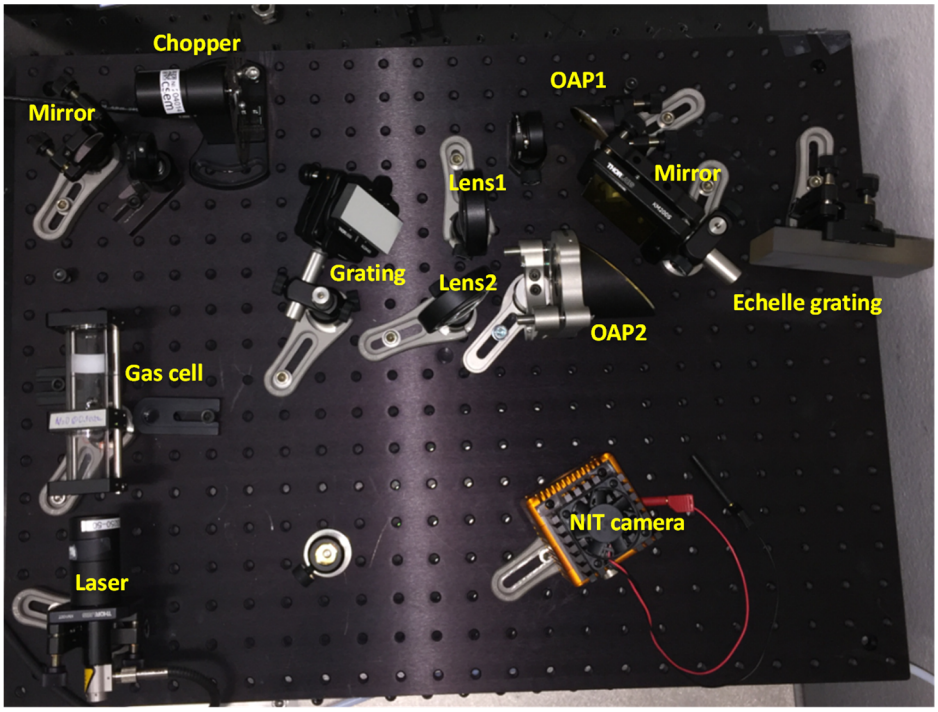

Figure 8: Experimental setup of 2D spectroscopy, using a combination of one echelle grating and one normal grating

The broadband supercontinuum collimated laser passed through the 10 cm-long gas cell before being expanded by the two off axis parabolic mirrors OAP1 and OAP2. The focal point is placed just underneath the square mirror. The expanded beam hits the echelle grating. Then, the reflected light from the echelle grating (in other words, wavelength dispersed light in vertical direction) is directed to a normal grating for a further dispersion in horizontal direction. The Lens 1 serves to collimate the beam, as it has been focused again by OAP2. Finally, the Lens 2 serves as a Fourier lens to resolve the dispersed light on the NIT camera. Consequently, the broadband light source turned to be spatially dispersed in 2 dimensions, which makes it

possible to perform a wide spectral range measurement, as shown in Figure 9. It is noteworthy that, in contrast to the VIPA based setup, only a portion of the camera pixels contribute to the absorption signal (compare Figure 5 to Figure 9).

We can see 6 distinct lines in y-axis. Each line corresponds to an individual transmission spectrum at different wavelength. As clearly seen, the spectrum at pixel #48 in x-axis experienced a strong gas absorption (See the yellow dotted circle in Figure 9), which was caused by the Q-branch of Methane at around 3315nm. Then, simply by computing the logarithmic ratio of the reference transmission spectrum to the spectrum that is measured at 40000 ppm of CH_4, the absorbance at the given gas concentration could be obtained.

To evaluate the performance of the trace gas sensing system, the transmission spectrum was measured every second as a function of CH_4 gas concentration from 1212 ppm to 40000 ppm 10 consecutive transmission profiles were measured for each concentration, in order to calculate the measurement repeatability. The standard deviation out of the 10 profiles were computed to demonstrate the system performance (See Figure 10).

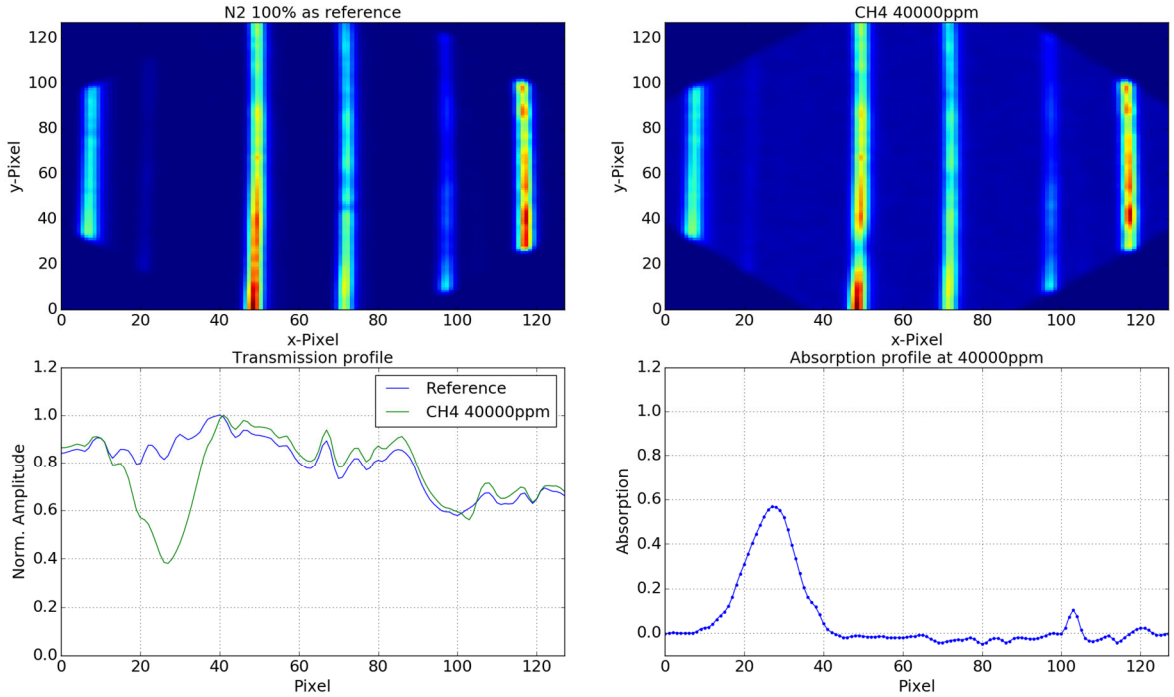

Figure 9: Measured CH_4 concentration at 40000ppm in a 10cm long cell, using echelle grating-based spectroscopy.

Let us discuss more details on the experimental results of the performance. Firstly, as expected, the measured concentration shows a good agreement with a theoretical exponential Beer-Lambert absorption curve, which proves the system linearity. Secondly, it is remarkable that the system noise was measured to be relatively small for low concentration at nominal 1212 ppm. This would correspond to a value around 24 ppm for a 10 m long multi-pass cell, considering 50% power loss due to reflection on the mirrors. We believe that the sensing system would be capable of measuring much lower concentration. However, the phenomenon that the absorption is saturated at about 0.52 instead of unity is abnormal. We believe that it would be attributed to the normalization issue when the transmission is computed. It seems that the noise floor level of the detector (NIT camera) is not same with and without the presence of the CH_4 gas inside the cell, even though it should not be the case. Then, it might lead to an offset in the computation of the transmission profile. Yet, it must be pointed out that this is totally related to the calibration issue and this offset can be readily compensated. In addition,

this offset doesn't influence the performance of the sensing system, since the measurement follows well the theoretically estimated curve.

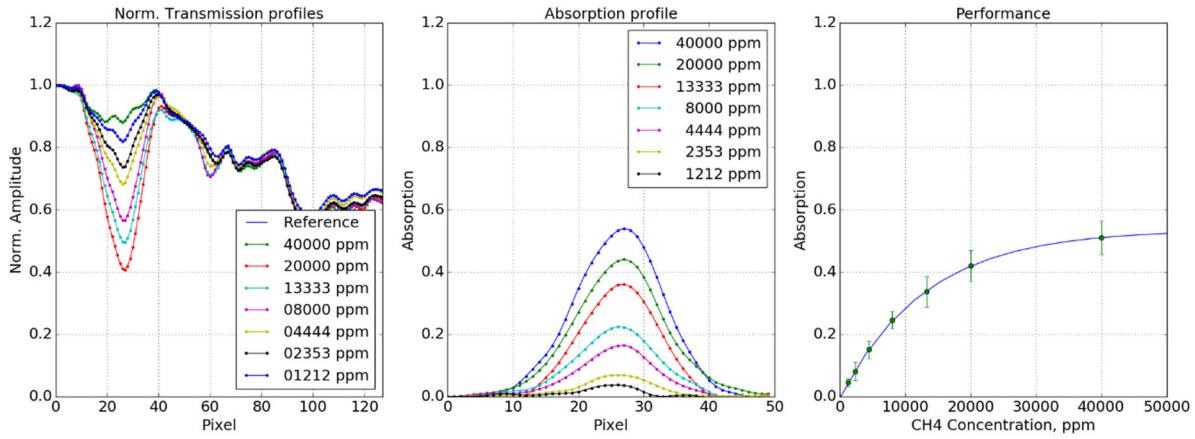

Figure 10: CH4 absorption profiles and the repeatability for different gas concentrations.

The spectral coverage and spectral resolution are not precisely known since it was not possible to clearly relate each of the 8 lines on the camera to a spectral region.

This system has a better sensitivity than the VIPA based setup, as expected, since the echelle grating introduces less losses than the VIPA. However, only a small portion of the 2D sensor is covered with valuable information, and even though the alignment is less critical than for the VIPA, the size and mass of the echelle grating makes it also more sensitive to vibrations and accelerations.

2.3 Single grating-based spectrometer with 2D array detector

When complication does not work, it is sometimes best to turn towards simple solutions.

2.3.1 Principle and Setup

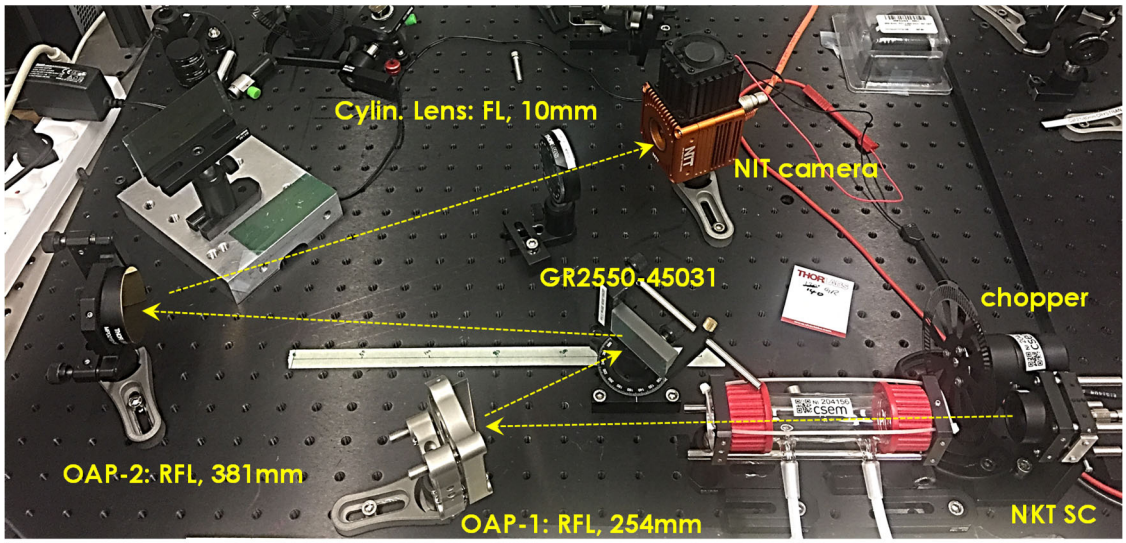

Figure 11: Single grating-based spectrometer.

Echelle grating-based spectrometer could improve the sensing performance, but it was still far from the target sensing sensitivity, which is a few ppm of CH_4. So, we decided to investigate another type of spectrometer, based on a single grating. Figure 11 illustrates the schematic diagram of the single grating-based spectrometer. The supercontinuum laser beam was

focused at the focal position of the off-axis parabolic mirror (OAP-1) by a Black Diamond-2 lens (BD-2, a chalcogenide made of an amorphous mixture of germanium (28%), antimony (12%), and selenium (60%)), while the 10 cm-long gas cell was placed in between the laser and the OAP-1. Then, the collimated beam reflected from OAP-1 hits the grating, so that the wavelength of the light is dispersed in horizontal direction. The 1st order reflected beam from the grating is focused on the camera after being reflected from the OAP-2. Since this configuration relies on a single grating, it could be considered as a 1D spectrometer.

To take the advantage of 2D array feature of the camera, one cylindrical lens was placed in front of the camera. So, the beam was expanded in vertical direction in front of the camera. This produces 2D image, as shown in Figure 12(left). The x-axis of the image represents the wavelength while the y-axis of the image represents replica of the transmission spectrum.

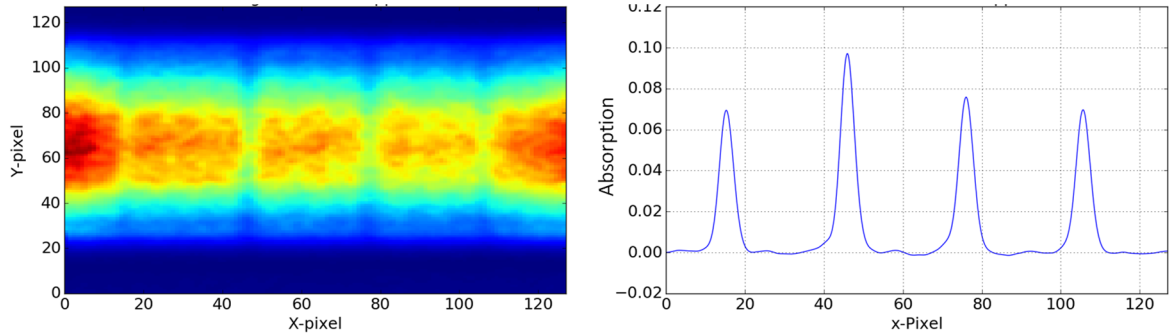

Figure 12: Image on the camera and CH_4 absorption profile at 4286 ppm.

This method has **2 crucial advantages** over the other 2D spectrometers:

1. The optical power at the camera is more intense than for 2D dispersed light, which improves greatly the SNR of the sensing.
2. All transmission profiles measured within each row are summed with weighting average as a final transmission profile (See Figure 13). This way the inherent white noise of the sensing system and the non-uniform gain fluctuation of pixels – an issue known for this type of detectors – could be significantly averaged out, resulting in a considerable improvement of SNR as well, without the need to perform non uniformity correction (NUC) at regular time intervals.

2.3.2 Experimental results

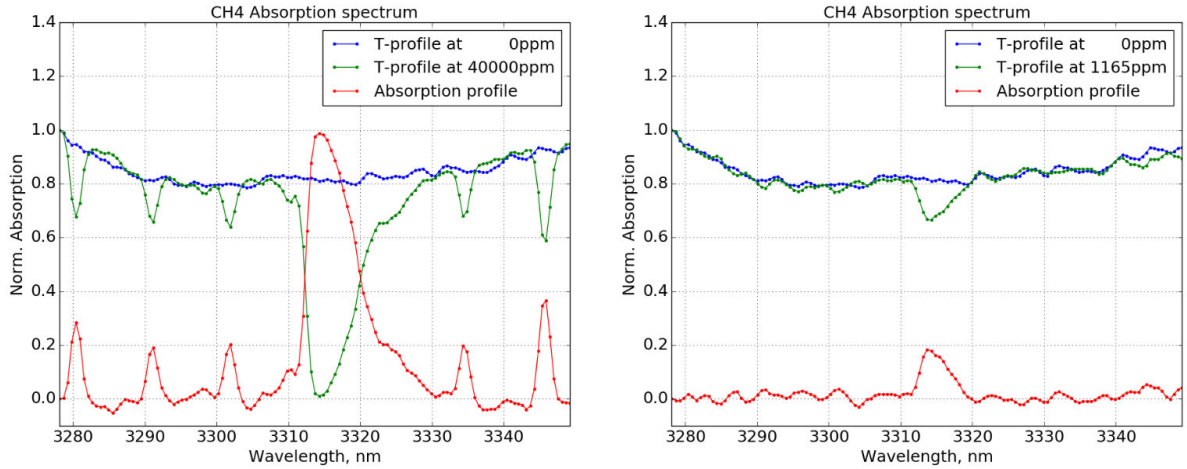

Figure 13: CH_4 concentration monitoring at 1165 ppm and 40000 ppm.

To evaluate the sensing performance of this system, the same experiment as described in §2.2.2 was repeated. Figure 13 demonstrates examples of the CH_4 gas absorption profile at two different concentration: 1126 ppm and 40000 ppm, showing a good SNR. Using HITRAN simulation, the x-axis of the camera image was calibrated to wavelength.

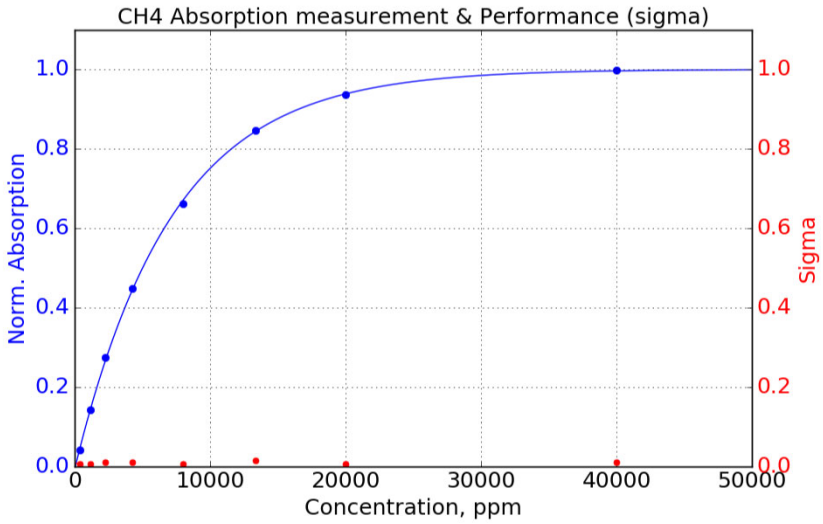

Figure 14: Performance of the single grating-based spectrometer.

Figure 14 clearly illustrates the generic characteristics of the sensing system performance. The methane absorption was measured from 40000 ppm down to 396 ppm. First, the measured concentrations match well the theoretical Beer-Lambert absorption curve, which proves the linearity of the sensing system. For each set concentration, the standard deviation out of 10 consecutive measurements was computed, which is nearly constant over the whole concentration range. It implies that the system noise is linear, and the sensor sensitivity is mainly limited by the system noise. In addition, the standard deviation is relatively small compared to the absorption amplitude at 396 ppm, showing approximately factor of 4. So, we believe that this sensing system might have a potential of monitoring as small as 100 ppm of CH_4 for a 10 cm-long absorption cell.

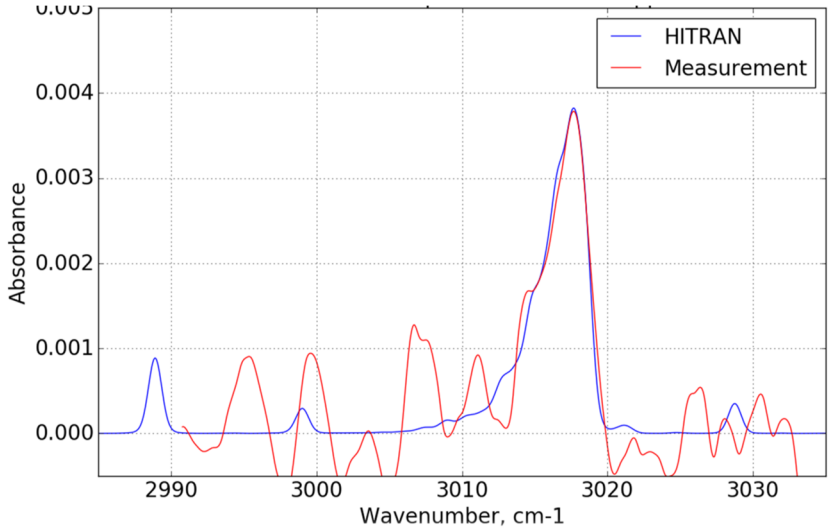

Figure 15: Absorption profile at CH4 50 ppm with 10 cm-long gas cell.

After upgrading the gas handling system, the CH_4 concentration could be further reduced to 50 ppm. However, a non-negligible noise oscillation starts to be visible on the spectrum (Figure

15), which corresponds to a SNR around 3. It seems that 50 ppm would be close to the sensing limit of this system for a 10 cm path length.

Apart from sensitivity, the spectral resolution is also an important parameter for the spectrometer. Indeed, in presence of a gas mixture, e.g. containing water vapor, it is important to distinguish the contribution of each components, by looking at absorption lines that are unaffected by the other gas species. Prior to the measurements, a Zemax simulation was performed, using the exact parameters of optics such as OPAs and grating (See Figure 16), which helped choosing an off-the-shelf grating. The theoretical spectral resolution and the measurement range of the spectrometer were estimated to be 0.5 cm^{-1} over 20 cm^{-1}, respectively.

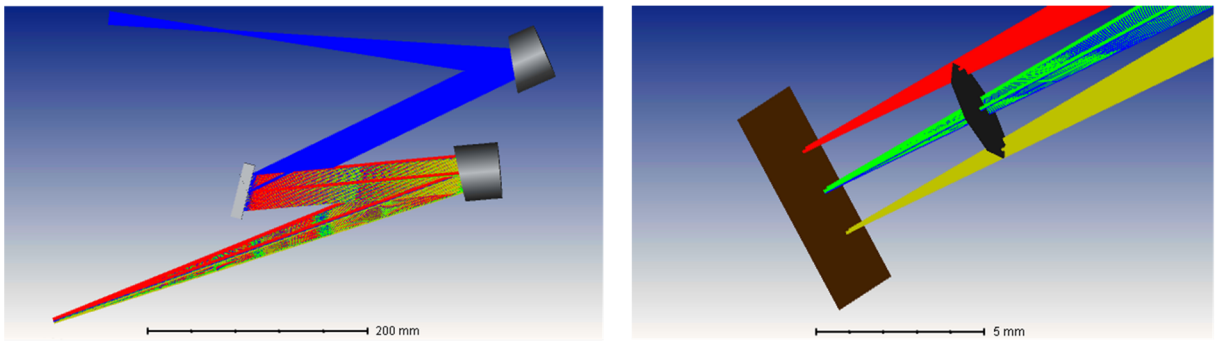

Figure 16: Zemax simulation to evaluate the spectral resolution of the single grating-based spectrometer

In order to validate the real resolution and bandwidth, the absorbance at 50 000 ppm concentration was then measured and compared to HITRAN simulations, as shown in Figure 17. The results are 0.6 cm^{-1} and 18 cm^{-1} respectively, which matches well with the Zemax simulation result. Notice that a larger spectral range measurement would be readily possible by multiple measurement while rotating the grating angle (See Figure 11).

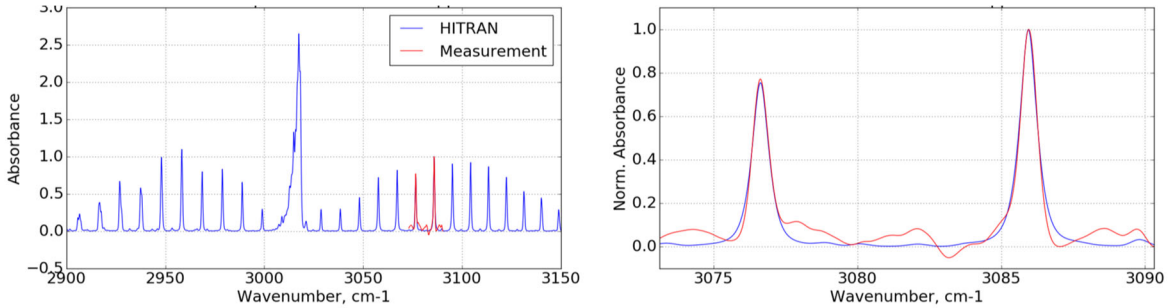

Figure 17: Measured spectral resolution of the single grating-based spectrometer.

So far, all the test experiments for CH_4 monitoring were performed with a 10-cm-long gas cell. However, in the final system, a ~10 m long multipass cell will be implemented, which will increase the light-gas molecule interaction length by a factor of 100, thus improving the detection sensitivity by the same factor, which corresponds to approximately 500 ppb for methane. This improvement is, of course, when only considering the interaction length increase. Losses due to multiple reflection on the MPC mirrors could degrade the SNR, thus raising the detection limit. At the time those tests were made, the MPC prototype was not yet available.

3 Conclusions

3 different types of spectrometers have been designed, assembled and their performance in terms of sensitivity and spectral resolution were evaluated, based on CH_4 concentration monitoring results. All 3 spectrometers suffer from the trade-off between sensitivity and spectral properties. However, among them, the consortium decided to continue with single grating-based spectrometer, since this spectrometer shows an encouragingly low limit of detection, acceptable spectral coverage and compatible spectral resolution. Moreover, the idea to spread the light vertically and perform averaging over the vertical pixel columns to overcome the non-uniformity issues of the matrix detector developed within the frame of this project has been regarded as particularly elegant.

It has also been decided to equip the grating with a motorized rotating platform to extend the detection range to match the broad supercontinuum spectrum, and allowing the detection of a larger number of gas species in successive screenshots.
Methane has been confirmed as the target gas for the demonstrations, with absorption measurements on the individual spikes near the Q-branch where water absorption wouldn't interfere too much.